JOURNAL OF MATERIALS SCIENCE 19 (1984) 3236–3248

The extraction of ionic conductivities and hopping rates from a.c. conductivity data

D. P. ALMOND
School of Materials Science, University of Bath, Bath, UK
C. C. HUNTER, A. R. WEST
Department of Chemistry, University of Aberdeen, Aberdeen, UK

Over a wide range of frequencies, the a.c. conductivity of ionic materials shows two regions of frequency-dependent conductivity. These are each characterized by a term $K\omega_p^{1-n}\omega^n$ where K, n are constants, ω_p is a fundamental frequency identified with the hopping rate and ω is the measuring frequency. This behaviour is an example of Jonscher's Law of Dielectric Response for ionic conductors. In many cases, the region of low-frequency dispersion approximates to a frequency-independent plateau which may be taken as the d.c. conductivity. In others, a significant low-frequency dispersion is present and cannot be ignored in determining the effective d.c. conductivity. A method for the extraction of d.c. conductivities, hopping rates and for estimating carrier concentration effects is described. Data for three different types of material, single-crystal $LiGaO_2$, β''-alumina and Na/Ag β-alumina are used to illustrate the method.

1. Introduction

Ionically conducting materials are currently being extensively investigated due, largely, to their potential value as solid electrolytes for novel batteries such as the sodium/sulphur cell. Their electrical characteristics are often studied by a.c. techniques to avoid the necessity of developing the non-blocking ion-conducting electrodes that are needed for d.c. measurements [1]. Many investigators use a.c. measurements simply to estimate the d.c. conductivity of ionic conductors. However, we have recently suggested [2, 3] that a.c. conductivity data can also be used to determine the hopping rates of ions in a conductor. This additional information is particularly valuable as it enables an assessment to be made of the relative importance of carrier mobility and mobile ion concentration in determining the net ionic conductivity of a particular material.

It is generally thought [4] that the a.c. conductivity $\sigma(\omega)$ of a hopping ion conductor takes the form

$$\sigma(\omega) = \sigma(0) + A\omega^n \quad (1)$$

at angular frequencies, ω, high enough to eliminate effects associated with electrode polarization or, in polycrystalline samples, grain boundaries. In Equation 1, $\sigma(0)$ corresponds to a frequency-independent plateau in $\sigma(\omega)$ which is usually identified with the d.c. conductivity of the material. At higher frequencies the conductivity increases as a power of frequency with the exponent $n < 1$. A relationship between $\sigma(0)$ and the a.c. coefficient A has been proposed [3] which may be used to estimate ion hopping rates from a.c. conductivity data alone. This relationship was derived, as a special case, for materials in which the a.c. conductivity is accurately frequency-independent at low frequencies and can be quantitatively described by Equation 1. Recent measurements [5] have shown that Equation 1 does not hold for the technologically important ionic conductor sodium–β''-alumina. This has prompted an extension of our analysis of a.c. conductivity to cover the determination of hopping rates in materials that do not exhibit frequency-independent conductivity plateaux and to indicate how estimates of d.c. conductivity may be obtained in such cases. An analysis of a.c. conductivity is presented

0022–2461/84 $03.00 + .12

in the next section and this is followed by examples of its application. Data from three materials, (a) sodium–β''-alumina, (b) $LiGaO_2$ and (c) an Ag/Na mixed alkali β-alumina, are examined. These examples cover the extremes of having (a) no conductivity plateau, and (b) a very well developed plateau. Example (c) is an intermediate case in which the data could be mistakenly analysed assuming a d.c. plateau.

2. Theory

A simple relationship between the coefficient A in Equation 1 and the d.c. conductivity $\sigma(0)$ was derived [2] by making the assumption that the two terms in Equation 1 were related to the same basic dielectric response of an ionic conductor in an a.c. field. Jonscher has proposed [6] that in hopping ion conductors the dielectric loss $\chi''(\omega)$ takes the Universal form

$$\chi''(\omega) \propto (\omega/\omega_p)^{n_1-1} + (\omega/\omega_p)^{n_2-1} \quad (2)$$

where ω_p is a characteristic frequency which in dipolar dielectrics is associated with the frequency of the dielectric loss peak. In conducting solids, dielectric loss and conductivity are related by

$$\chi''(\omega) \equiv \sigma(\omega)/\epsilon_0\omega \quad (3)$$

An expression for a.c. conductivity, of the same form as Equation 1, can be obtained from Equations 2 and 3 for the special case in which $n_1 = 0$ and $n_2 = n$

$$\sigma(\omega) = K\omega_p + K\omega_p^{1-n}\omega^n \quad (4)$$

and where K is the constant of proportionality which will be identified later.

If ω_p is identified with the ion hopping rate and this is assumed to be thermally activated with an activation energy E_a, Equation 4 may be re-expressed as

$$\sigma(\omega) = K\omega_e \exp(-E_a/kT) + K\omega_e^{1-n} \exp[-(1-n)E_a/kT]\,\omega^n \quad (5)$$

Hence the a.c. coefficient A is predicted to be thermally activated with an activation energy $(1-n)E_a$ and to have a magnitude which is related to the d.c. conductivity by

$$A = \frac{\sigma(0)}{\omega_p^n} \text{ and } \lim_{T\to\infty} \frac{\sigma(0)}{A} = \omega_e^n \quad (6)$$

in Equations 5 and 6, ω_e is an effective attempt frequency [2] which includes an entropy term:

$$\omega_e = \exp(\Delta S/k)\omega_0 \quad (7)$$

where ΔS is the entropy of activation, ω_0 is a lattice vibrational frequency and k is Boltzmann's constant. The parameters included in K may be obtained from the expression for d.c. conductivity [7]

$$\sigma(0) = K\omega_p = [Ne^2a^2/kT]\gamma c(1-c)\omega_p \quad (8)$$

where γ is a geometrical factor that may include a correlation factor, c is the concentration of mobile ions on N equivalent lattice sites per unit volume, a is the hopping distance and e is the electronic charge. The concentration of mobile ions c may, in some conductors, also be thermally activated and contribute to the net temperature dependence of the conductivity [3].

Measurements, using mechanical relaxation and infrared absorption techniques, have been made [8, 9] of the hopping rates and attempt frequency of the widely studied superionic conductor sodium–β-alumina. Consequently, a.c. conductivity data for sodium–β-alumina were chosen to test the predictions, Equations 5 and 6, of this new analysis. The frequency-independent plateaux found in the data provided estimates of d.c. conductivity which were in good agreement with measurements obtained using non-blocking electrodes [10] and the relationships, Equations 5 and 6, between a.c. and d.c. conductivities were shown to hold [2].

Ion hopping rates may be obtained in a particularly simple way from Equation 4 which may be rewritten as

$$\sigma(\omega) = K\omega_p[1 + (\omega/\omega_p)^n] = \sigma(0)[1 + (\omega/\omega_p)^n] \quad (9)$$

Now the hopping rate can be found by inspection of the a.c. conductivity data since $\omega_p = \omega$ when

$$\sigma(\omega) = 2\sigma(0) \quad (10)$$

The relationships between a.c. and d.c. conductivity are shown schematically in Fig. 1.

As mentioned in Section 1, the assumption that the a.c. response of a conductor could be represented by Equation 1 was found to be inapplicable to the a.c. conductivity data obtained for sodium–β''-alumina. Some of these data are shown in Fig. 2. Instead of a frequency-independent plateau in conductivity at low frequencies, a continual increase in conductivity is observed followed, at higher frequencies, by the usual dispersion. The equivalent dielectric loss associated with this

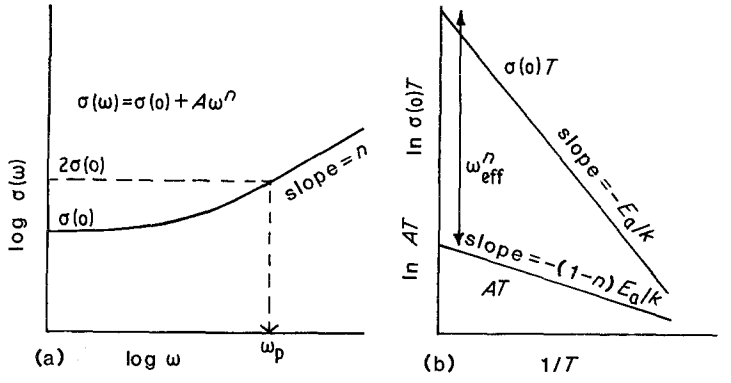

Figure 1 Characteristic of the a.c. conductivity of materials for which $n_1 = 0$, no low-frequency dispersion, is a good approximation. A method of estimating ω_p is shown in (a) and the temperature dependence of a.c. and d.c. terms is shown in (b).

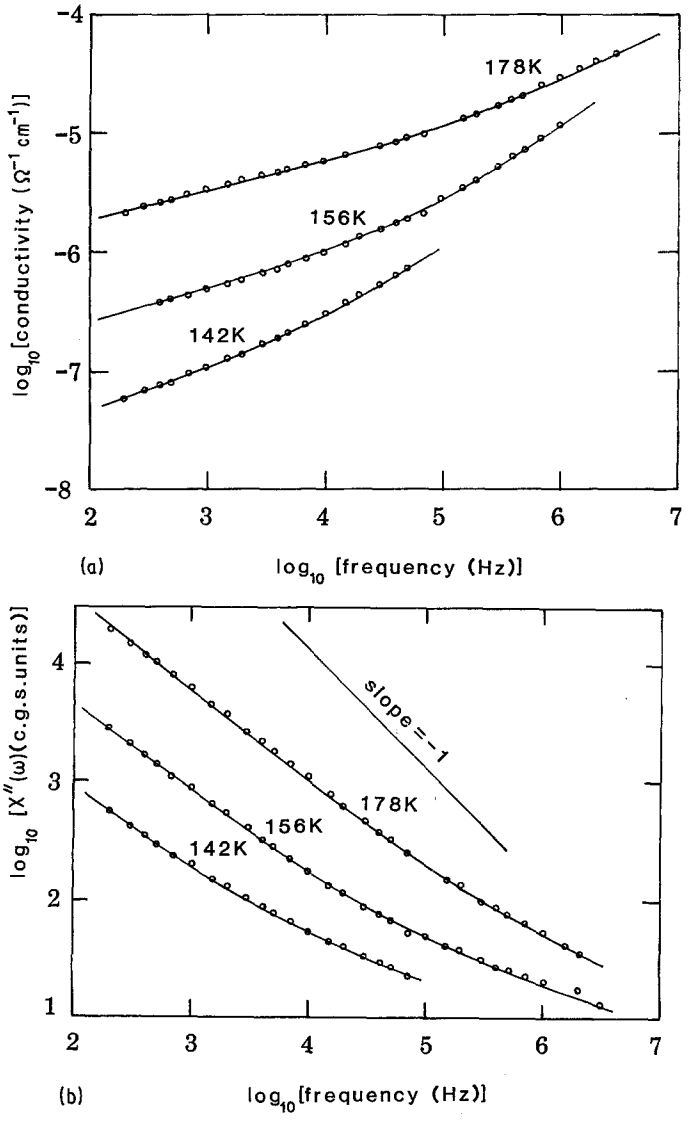

Figure 2 Measurements of the a.c. conductivity (a) and dielectric loss (b) of single-crystal sodium–β''-alumina.

behaviour is also shown in Fig. 2. At low frequencies it has a slope less than -1 and, as such, is an example of the low-frequency dispersion [11, 12] encompassed by the universal response function Equation 2 with $n_1 \neq 0$. For materials that exhibit significant low-frequency dispersion, the absence of a low-frequency conductivity plateau brings into focus the validity of using a.c. data to obtain reliable estimates of d.c. ionic conductivity.

The general expression for the a.c. conductivity of a material which exhibits both low- and high-frequency dispersion may be derived from Equations 2 and 3 assuming $n_1 \neq 0$:

$$\sigma(\omega) = K\omega_p^{1-n_1}\omega^{n_1} + K\omega_p^{1-n_2}\omega^{n_2}. \quad (11)$$

In general, when $\omega = \omega_p$ both terms in Equation 11 are equal to the d.c. conductivity, $K\omega_p$; ω_p and $\sigma(0)$ may be extracted from the data by inspection using one of the methods indicated in Fig. 3. Equation 11 simplifies to Equation 4 in cases where $n_1 = 0$ and if it can be assumed that the components of K are the same as those given in Equation 8 for d.c. conductivity. As is shown in the three analyses that follow, the condition $n_1 = 0$ may not be observed experimentally. Instead, small positive values of n_1 are needed to accurately describe the experimental data.

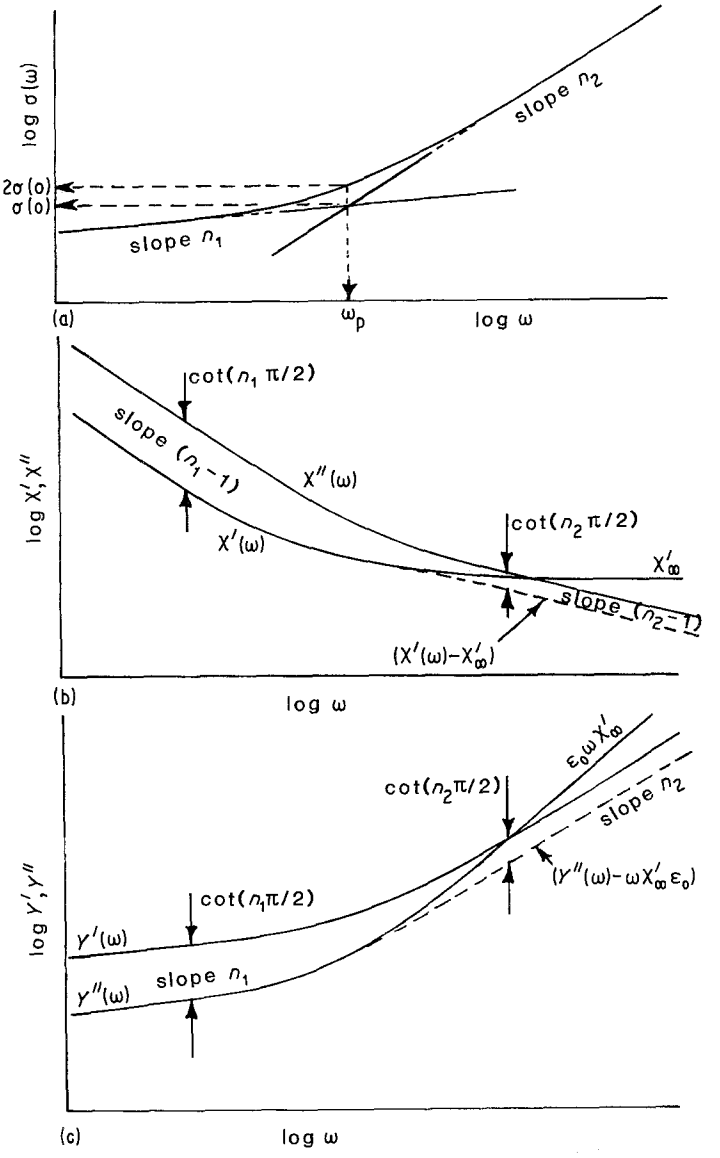

Figure 3 Characteristics of the a.c. conductivity (a), the two components of the dielectric constant (b), and the complex admittance (c) of materials exhibiting significant low-frequency dispersion. A method of estimating ω_p and $\sigma(0)$ from a.c. conductivity data is indicated in (a) and the relationships, Equations 12, 15 and 17, are illustrated in (b) and (c).

The low-frequency dispersion, or "creeping d.c. conductivity" [12], is not to be confused with the familiar polarization effects found at low frequencies, caused by the use of blocking electrodes. Low-frequency dispersion appears to be an integral part of the dielectric response of an ionic conductor. Its close relationship, in most cases, to the conductive response is not unexpected as at low frequencies the ions respond by moving bodily, by a sequence of activated hops, towards the appropriate electrode. This translation of charge within the bulk of the conductor therefore produces an increase in permittivity. The low-frequency dispersion in the dielectric loss $\chi''(\omega)$ necessitates [6] a similar power-law dispersion in the real part of the dielectric constant $\chi'(\omega)$ and the magnitudes of the two components are connected, because of the Kramers–Kronig relationships, by

$$\chi''(\omega)/\chi'(\omega) = \cot(n_1\pi/2) \qquad (12)$$

These relationships between the magnitudes of the two components are also shown in Fig. 3. Conventional electrode polarization effects also produce increases in permittivity but these are accompanied by a rapid decrease in conductivity with decreasing frequency. Their presence leads to a breakdown of the relationship, Equation 12, between $\chi'(\omega)$ and $\chi''(\omega)$ as will be illustrated by the examples which follow this section.

The acceptance of the presence of two dispersive terms in the a.c. conductivity raises problems in justifying the use of a.c. techniques for determining d.c. conductivities. The supposed d.c. term in Equation 1, is now a second frequency-dependent term. In the majority of cases its frequency-dependence appears to have been very weak and this second contribution to the dispersion has gone unnoticed. Nevertheless, in our test material, sodium–β-alumina, relationships based on the assumption that the apparent d.c. term was, in fact, a low-frequency dispersion term with a very small exponent, have been confirmed experimentally. The critical frequencies from the electrical data were shown to agree with those obtained, in quite a different way, from mechanical relaxation measurements and the d.c. plateau values were found to be consistent with true d.c. conductivity measurements. It is concluded that there are no separate a.c. and d.c. contributions to conductivity and that the d.c. conductivity amounts to the limiting case of the general a.c. response, characterized by Equation 2. These, and other questions raised by this analysis will be taken up again later.

The electrical properties of ionic conductors have traditionally been analysed using equivalent circuits [1]. These circuits usually include a number of parallel RC elements and as a result the admittance formalism is often employed for the representation of experimental data. Note that the complex admittance, Y^*, may be regarded as the complex conductivity, σ^*. Hence the real part of the admittance Y' equals the conductivity σ. The bulk response of a conductor exhibiting the high- and low-frequency dispersions discussed here may be represented by the equivalent circuit shown in Fig. 4. This differs from the circuit employed previously [13] to explain the data obtained from sodium–β-alumina in that the parallel resistive element, which represented the frequency-independent conductivity plateau, has been replaced by a second dispersive element. This second element contributes to both conductivity and permittivity, to simulate the effects of low-frequency dispersion. The admittance of the equivalent circuit is

$$Y^*(\omega) = A_1\omega^{n_1} + A_2\omega^{n_2} + i(B_1\omega^{n_1} + B_2\omega^{n_2}) + i\omega C_\infty \qquad (13)$$

in which C_∞ is the infinite frequency capacitance and the parameters A_1, B_1, A_2 and B_2 are given by the relationships

$$A_1 = K\omega_p^{1-n_1} \qquad (14)$$

$$B_1 = A_1\tan(n_1\pi/2) \qquad (15)$$

$$A_2 = K\omega_p^{1-n_2} \qquad (16)$$

$$B_2 = A_2\tan(n_2\pi/2) \qquad (17)$$

The behaviour of the real and imaginary parts of the admittance are also shown in Fig. 3.

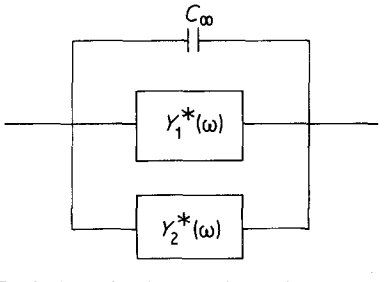

Figure 4 Equivalent circuit to model the bulk a.c. behaviour of ionic conductors which shows low-frequency dispersion.

3. Analysis of experimental results

3.1. Sodium–β''-alumina

A.c. conductivity measurements of a single-crystal sample† of Naβ''-alumina are shown in Fig. 5a. These measurements, and those discussed in other parts of this section, were obtained using admittance bridge techniques [14] and ion-blocking gold electrodes. The three phenomena: high-frequency dispersion, low-frequency dispersion, and electrode polarization are evident in the conductivity data. The two distinct regions of low- and high-frequency dispersion, displayed most clearly in the 178 K data, are also present in the lower temperature data sets. At 208 K, however, the high-frequency dispersion is absent and a rapid fall in conductivity is found at low frequencies. This is distinctly different to the gradual change, spread over several decades of frequency, associated with low-frequency dispersion and is typical of electrode polarization. The slope of the plots of log σ against log f in this region ≈ 1, which compares with the value of 2 expected for an electrode response that may be simulated by a Debye-like series RC element. The change in the conductive response from low- to high-frequency dispersion occurs where $\omega \approx \omega_p$, Equation 2. As ω_p is thermally activated, this region shifts to higher frequencies with increasing temperature and finally, at temperatures of ≈ 208 K and higher, falls outside the range of these measurements.

The two components of the permittivity $\chi^*(\omega)$ and the admittance $Y^*(\omega)$, of some of the data sets, are shown in Figs. 5b and c. The effects of the limiting infinite frequency permittivity, χ_∞, of the sample on $\chi'(\omega)$ and $Y''(\omega)$ are indicated. The 178 and 156 K results seem to adhere to the Kramers–Kronig relationships, Equation 12, at both high and low frequencies. It has been suggested [15] that the exponents n_1 and n_2 for the two dispersions can often be accurately determined by using Equation 12. This procedure was adopted with success here. The values of both exponents were found to decrease with temperature. This behaviour is reminiscent of the increase in the high-frequency exponent n_2 found in sodium–β-alumina at temperatures below ≈ 120 K [2]. It was suggested that this correlated well with the NMR evidence [16] for the formation of ordered microdomains of Na^+ ions at similar temperatures in sodium–β-alumina. In sodium–β''-alumina there is evidence for microdomain formation in the 150 to 190 K temperature range [17] which suggests that the changes in n_1 and n_2 found here, may also be attributed to ordering of Na^+ ions.

The low-frequency dispersion in the 208 K data is terminated at low frequencies by the appearance of a competing electrode polarization phenomenon. This causes a steeper rise in $\chi'(\omega)$ at low frequencies below $\approx 10^4$ Hz, accompanied by a decrease in $\chi''(\omega)$ due to a reduction in the effective field across the sample caused by the polarization reducing the measured a.c. current. Again these electrode polarization effects are quite unlike the low-frequency dispersion exhibited at low frequencies in the 178 K data. Having established that much of the conductive response (Fig. 5a) is characteristic of the bulk dielectric properties of sodium–β''-alumina, it is legitimate to proceed to extract estimates of d.c. conductivities and hopping rates using the techniques outlined above.

It is evident from Equation 11 or Fig. 3 that ion hopping rates and conductivities can be obtained from a.c. conductivity data provided the frequency range of the data covers the region in which the response changes from the low- to the high-frequency dispersion. Of the sodium–β''-alumina data shown in Fig. 5a only the 178 and 156 K data clearly satisfy this requirement, though the 142 K data may, with some reservations, also be used. In each of these cases the low-frequency region has been extrapolated to determine the frequency at which it produces a contribution of equal magnitude to the high-frequency dispersion component, as in Fig. 3. The values of d.c. conductivity and hopping rates obtained in this way are shown plotted in an Arrhenius fashion in Fig. 5d. In addition a conventional complex impedance plot analysis [1] was used to provide estimates of the d.c. conductivity of the higher temperature data. These values appear to be lower than would be obtained by an extrapolation of the low-temperature data. Possible reasons for this discrepancy between conductivities obtained by these two methods of analysis, will be discussed later. Despite the small number of points it seems that the conductivity and hopping rates are both controlled by the same activation energy. This activation energy of ≈ 0.25 eV compares favourably with the

†Flux grown crystal provided by B. Wanklyn of Clarendon Laboratories Oxford University.

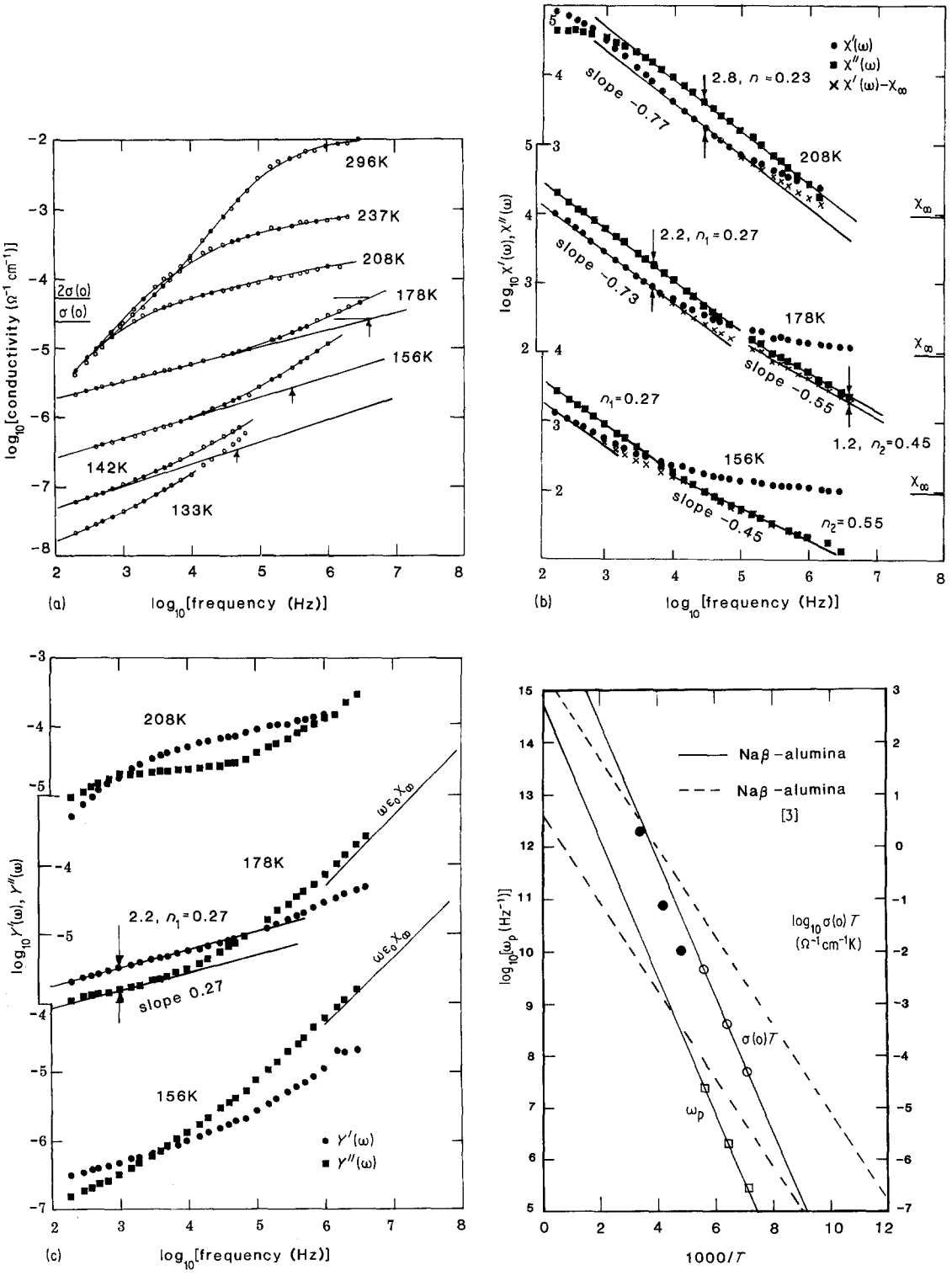

Figure 5 Measurements of the a.c. conductivity (a), the dielectric loss and dielectric constant (b), and the components of the complex admittance (c) of single crystal sodium–β''-alumina. Estimates of ionic hopping rate, ω_p, and d.c. conductivity are shown plotted in an Arrhenius fashion (d). Similar results [3] for Naβ-alumina are indicated for comparison.

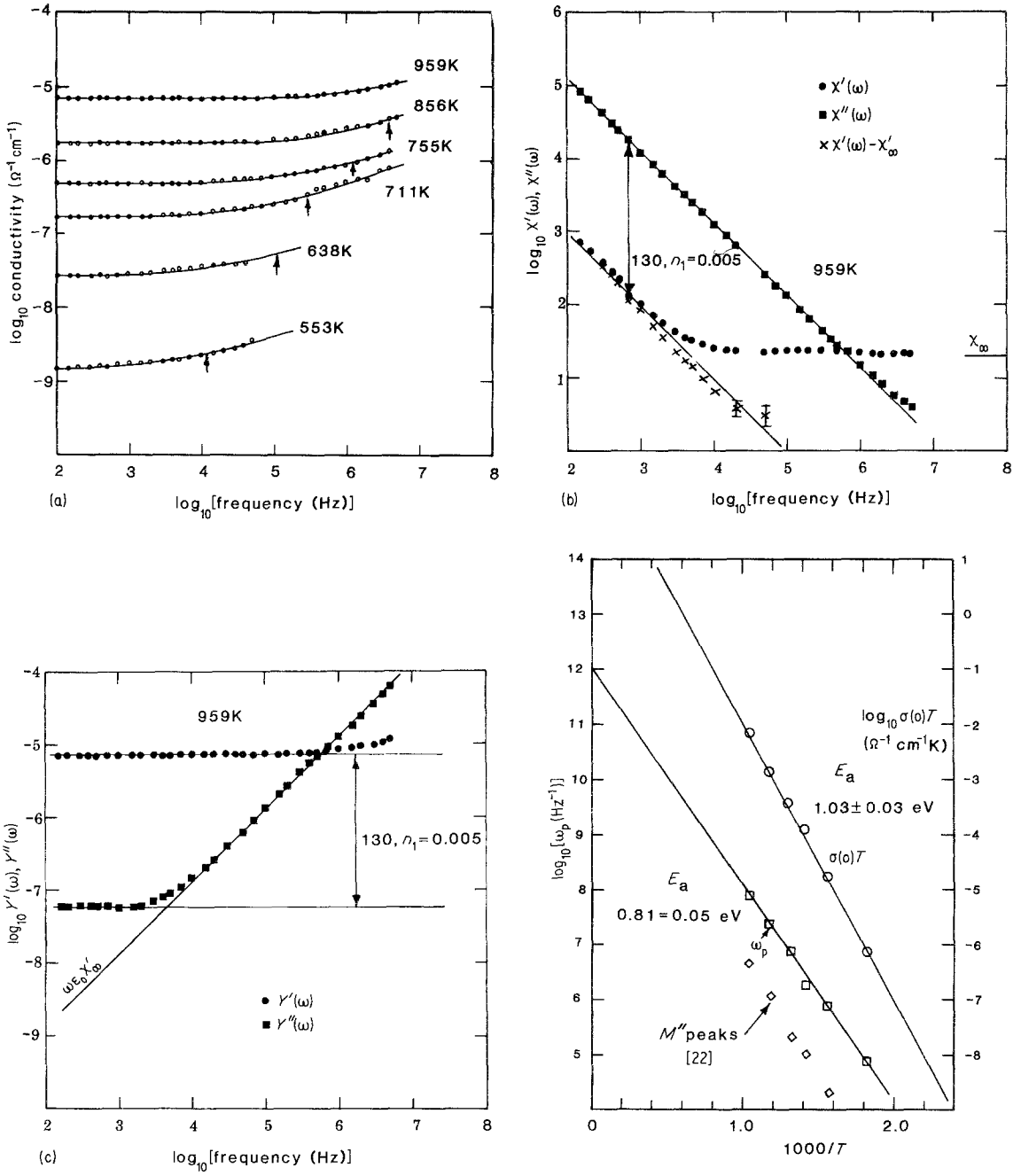

Figure 6 Measurements of the a.c. conductivity (a), the dielectric loss and dielectric constant (b), and the components of the complex admittance (c) of single-crystal lithium gallate. Estimates of ionic hopping rate, ω_p, and the d.c. conductivity are shown plotted in an Arrhenius fashion in (d). Also shown are the frequencies of the complex electric modulus peaks [22].

values obtained by other workers [18, 19] for single-crystal samples of sodium–β''-alumina at low temperatures.

The magnitude of the constant K ($K = \sigma/\omega_p$) which is largely a measure of the mobile ion concentration is $\approx 1.5 \times 10^{-12}\,\Omega^{-1}\,cm^{-1}\,Hz^{-1}$ which may be compared with the value $5 \times 10^{-12}\,\Omega^{-1}\,cm^{-1}\,Hz^{-1}$ obtained for single-crystal sodium–β-alumina at similar temperatures [3]. Much of the difference between these two values can be accounted for by the shorter hopping distance a, for sodium–β''-alumina, which appears as a^2 in

Equation 8 for $\sigma(0)$. It is concluded that the mobile ion concentration in sodium–β''-alumina is very similar to the $\approx 20\%$ deduced [3] for sodium–β-alumina. $\sigma(0)T$ and ω_p obtained from sodium–β-alumina data are also shown in Fig. 5d. Despite the apparently lower value of K the conductivity of sodium–β''-alumina exceeds that of sodium–β-alumina at high temperatures. It is, in fact, widely recognized [20] that sodium–β''-alumina is the better ionic conductor at high temperatures and, because of this, commercial electrolytes are produced in a predominantly β''-alumina form. Our results indicate that this high conductivity must be attributed to a comparatively higher ion hopping rate in sodium–β''-alumina. This, in turn, may be traced to the large difference in effective attempt frequencies and, through Equation 8, to a larger "effective" entropy of activation for β''-alumina.

3.2. $LiGaO_2$

A.c. conductivity measurements [21] of single-crystal $LiGaO_2$ are shown in Fig. 6a. In sharp contrast with Naβ''-alumina, Fig. 5a, frequency-independent conductivity plateaux are found ir the $LiGaO_2$ data at lower frequencies. The two components of the measured complex permittivity $\chi^*(\omega)$ and complex admittance $Y^*(\omega)$ are shown for the 959 K data in Figs. 6b and c. The real part of the permittivity, Fig. 6b, clearly tends towards a high-frequency limiting value, χ_∞, of 21. When this is subtracted from $\chi'(\omega)$ data, the frequency-dependent part, within experimental errors, decays with the same power law as $\chi''(\omega)$. This is an inevitable consequency of the Kramers–Kronig relationships which, because of the relationship, Equation 2, between $\chi'(\omega)$ and $\chi''(\omega)$, also implies a non-zero low-frequency dispersion in the conductivity. In the case of $LiGaO_2$ the ratio of $\chi'' : \chi'$ is about 130, compared to about 2 for sodium–β''-alumina, and equating this with $\cot n_1 \pi/2$ yields a value for n_1 of 0.0055. A low-frequency dispersion in conductivity with such a tiny power-law exponent is indistinguishable, within experimental error, from a frequency-independent plateau. The high temperature data were chosen for display in Figs. 6b and c because in these the apparent plateau was best developed and because in these the largest change in $\chi'(\omega)$ is found. At lower temperatures $\chi''(\omega)$ decreases with $\sigma(\omega)$ and as a result so does the frequency-dependent part of $\chi'(\omega)$. The value $\chi_\infty \approx 21$ is, however, comparatively large and relatively independent of temperature. At lower temperatures it "swamps" the frequency-dependent part of $\chi'(\omega)$ and the response could be mistaken for electronic conduction with frequency-independent conductivity and permittivity.

Ion hopping rates were obtained from the conductivity data Fig. 6a using the approximate relationship, valid for zero low-frequency dispersion, Equation 10. Values of hopping rate ω_p and d.c. conductivity are shown plotted in an Arrhenius fashion in Fig. 6d. The hopping rate appears to be controlled by a distinctly lower activation energy than that of the total conductivity. It is concluded [3] that the carrier concentration is thermally activated in $LiGaO_2$ with an activation energy of about 0.2 eV. The magnitude of the carrier concentration factor K ($K = \sigma(0)/\omega_p$) varies between $\approx (1.5 \text{ and } 7) \times 10^{-14}\ \Omega^{-1}\,\text{cm}^{-1}\,\text{Hz}^{-1}$ which is about two orders of magnitude lower than found in sodium–β-alumina. $LiGaO_2$ has a well ordered crystal structure in which Li^+ ion conduction is thought [22] to occur by interstitial diffusion. It seems reasonable to suppose that the number of interstitial carriers should be thermally activated and that the activation energy for carrier creation should be about 0.2 eV. In contrast to sodium–β''-alumina, a much lower effective attempt frequency for ionic hopping, $\approx 10^{12}$ Hz, is indicated by the $LiGaO_2$ data. This shows that the entropy of activation is small in $LiGaO_2$ which again seems reasonable for the interstitial diffusion of the small number of Li^+ ions through an otherwise well ordered crystal structure.

A possible consequence of χ_∞ dominating part o of the electrical response has already been mentioned. A further consequence of this can be seen by comparing, in Fig. 6d, the frequencies of complex electric modulus, $M''(\omega)$, peaks [22] with ω_p values. The complex electric modulus formalism, $M^*(\omega)$, has been used by a number of workers [23, 24] as a method of analysing electrical response data. The imaginary part $M''(\omega)$ has appeared to have been useful because it passes through a peak, as a function of frequency, which is thermally activated with a similar activation energy to the conductivity. It has been tempting to attribute physical significance to the peak frequency in the same way that one might to a dielectric loss peak frequency. However, we have recently analysed the electric modulus notation [25], using some of the results outlined here, and found the peak frequency to depend strongly on the relative mag-

nitudes of χ_∞ and K. In $LiGaO_2$ the capacitive response is dominated by χ_∞ whilst the conductive response is attributed to the quite different physical process of ion diffusion. It is not surprising, therefore, that the $M''(\omega)$ peak frequencies are not related in a simple way, as is found for dielectric loss or internal friction peaks, to the ionic hopping rate, ω_p. Finally, in $LiGaO_2$, K is thermally activated and the ratio of χ_∞ to K changes with temperature. As a result the relationship between ion hopping rate ω_p and $M''(\omega)$ peak frequency [25] is temperature-dependent and an activation energy obtained from $M''(\omega)$ peaks has no physical significance.

3.3. Na/Ag β-alumina

A.c. conductivity measurements [26] of our third example, a mixed Na/Ag single-crystal sample of β alumina, are shown in Fig. 7a. This data set has been chosen because the low-frequency dispersion is less pronounced than in sodium–β″-alumina and it might be mistaken for a frequency-independent conductivity plateau. Two methods have been used to extract ω_p values. First, the points that would be used to estimate ω_p, using Equation 9 where $\sigma(\omega) = 2\sigma(0)$, are indicated by the upper arrows. In the absence of good frequency-independent plateaux the choice of $\sigma(0)$ becomes uncertain, but for the purpose of this illustration the lowest measured were used. Second, the components of the complex permittivity $\chi^*(\omega)$ and complex admittance $Y^*(\omega)$, measured at 328 and 215 K are shown in Figs. 7b and c. As before, χ_∞ has been subtracted from $\chi'(\omega)$ in Fig. 7b to demonstrate a low-frequency dispersion in both components. The relationship between the magnitudes of $\chi'(\omega)$ and $\chi''(\omega)$, Equation 12, was used to estimate n_1. In this case $n_1 \approx 0.05$ at higher temperatures rising to ≈ 0.09 at the lower temperatures. These values were then used to obtain estimates of ω_p and $\sigma(0)$ by the same procedure as adopted for the sodium–β″-alumina data. The lower arrows indicate the frequencies at which $\omega = \omega_p$. These are seen to be over an order of magnitude higher than obtained incorrectly, using the approximate relationship, Equation 9.

Estimates of the d.c. conductivity and ion hopping rate are shown plotted in an Arrhenius fashion in Fig. 7d. Both appear to be thermally activated with an activation energy of ≈ 0.035 eV. Details of the mixed alkali effect [27] in this Na/Ag system have been published elsewhere [26]. The sample was a sodium–β-alumina single crystal which was ion exchanged with silver until 40% of the sodium ions had been replaced by silver ions. The increase in activation energy for ionic conduction from 0.16 eV for pure sodium–β-alumina, to 0.35 eV for the mixed alkali is typical of such systems. It is notable, however, that the pre-exponential factor, σ_0, the infinite temperature intercept of $\sigma(0)T$ in Fig. 7d, is little different from the sodium–β-alumina value, Fig. 5d. This might be interpreted as evidence of little change in mobile ion concentration with ion exchange. However, the carrier concentration parameter K for this mixed alkali, calculated using the values of ω_p shown in Fig. 7d, is only $\approx 5 \times 10^{-13}\ \Omega^{-1}\ cm^{-1}\ Hz^{-1}$ which is an order of magnitude lower than estimated for sodium–β-alumina. This low K value is compensated for, in the pre-exponential factor σ_0, by an increase in effective attempt frequency attributable to an increase in the effective entropy of activation for the more disordered system.

The two main conclusions, that mobile ion concentration is reduced and hopping rate increased with ion exchange, find some support in observations of other mixed alkali systems. A weak electrolyte theory has been employed [28] to explain the mixed alkali effect in Na/K β-alumina. It has been argued that mobile ion concentration can be reduced by the formation of immobile Na^+–K^+ ion pairs and similar arguments have been developed for the Na/Ag system [5]. In Na/Li β-alumina both NMR and internal friction estimates of hopping rate [29] show comparatively little change with ion exchange, despite a significant increase in activation energy [30], indicating a compensating increase in effective attempt frequency.

4. Discussion and conclusions

The preceding analyses have demonstrated the potential value of detailed a.c. response measurements in characterizing the conductivities of ionic conductors. The ability to extract an ion hopping rate leads to the possibilities (i) of carrier concentration estimation, or comparison, (ii) of detecting variations of carrier concentration with temperature and (iii) of estimating the importance of the entropy of activation. All of these possibilities are dependent on the validity of Equation 2 for the Universal dielectric response of a hopping ion conductor. The presence of two power-law response mechanisms, the low- and high-frequency

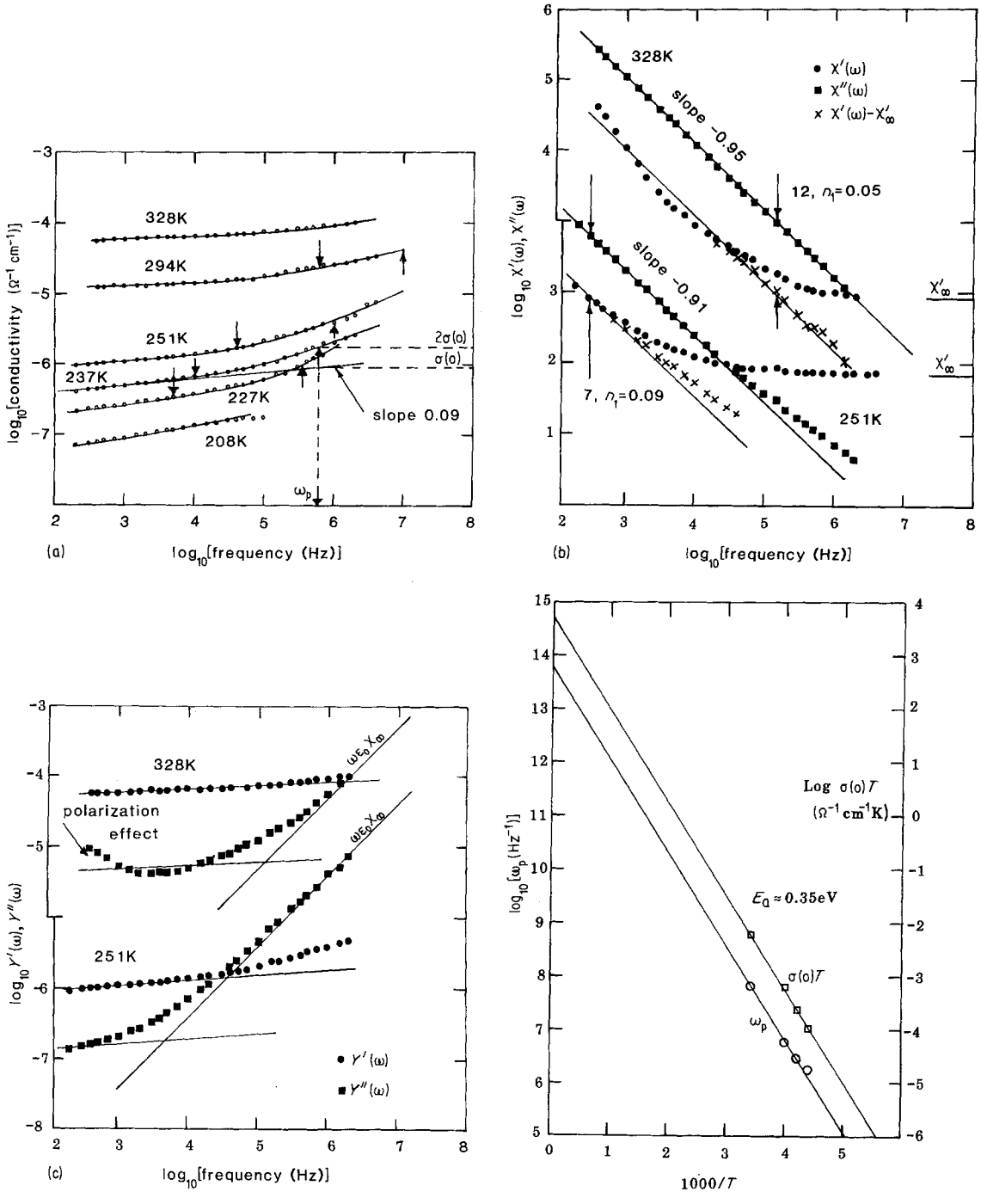

Figure 7 Measurements of the a.c. conductivity (a), the dielectric loss and dielectric constant (b), and the components of the complex admittance (c), of single-crystal mixed alkali $Ag_{0.4}$, $Na_{0.6}$ β-alumina. Estimates of ionic hopping rate, ω_p, and the d.c. conductivity are shown plotted in an Arrhenius fashion in (d).

dispersions, has been adequately confirmed by this and other work. Indeed, even in the unlikely case of $LiGaO_2$ it must be concluded that low-frequency dispersion is present. What has not been experimentally confirmed other than in Naβ-alumina [2] is that the two terms should contribute, as suggested in Equation 2, in equal measure. In sodium–β-alumina, it has been found that values of ω_p derived from a.c. conductivity, using the methods of analysis developed here, are in good agreement with those obtained independently by mechanical relaxation measurements. Similar electrical/mechanical studies of other materials would be of great value for investigating the general validity of the relationships employed here.

The physical origins of the two dispersions found in the conductive and dielectric responses of ionic conductivities have been discussed by Jonscher [11, 31]. The high-frequency dispersion occurs where $\omega > \omega_p$ and the response is essentially the same as that of a dipolar dielectric. In this regime the power-law dispersion is attributed [32, 33] to the presence of many-body excitations in the ionic system. These excitations perform the required readjustments of the ionic environment of an ion after it arrives, by a thermally activated hopping event, at a new site. The low-frequency dispersion occurs where $\omega < \omega_p$ and the response is conductive, involving the translation of ions within the conductors as was explained earlier. Jonscher has suggested [11] that the dispersion may be caused by the presence of impurities and crystalline imperfections that impede the progress of ions through a lattice. Recently, Yoshikado *et al.* [34, 35] have shown that the low-frequency dispersion in hollandite is dependent on crystalline perfection. Dissado and Hill [36], however, by a development of their many body theory of dipolar dielectrics [33], predict the presence of low-frequency dispersion in ionic systems where ionic motion is restricted to one or two dimensions.

The d.c. conductivity of an ionic conductor, $K\omega_p$, obtained as illustrated in Fig. 3, may be interpreted as being the potentially achievable conductivity of the system in the absence of imperfections. The difference between the complex plane estimates and $K\omega_p$ values for sodium–β''-alumina, shown in Fig. 5d, may perhaps be evidence of this distinction between "real" and achievable conductivities.

The main objective of this work has been to develop a technique for the extraction of ion hopping rates from a.c. conductivity data. The results obtained for sodium–β''-alumina and Ag/Na β-alumina, however, seem to raise questions about the meanings of such concepts in high-density ionic systems. In both cases the apparent hopping rates are anomalously high suggesting large entropies of activation. This concept, and the basic equation for ionic conductivity, Equation 8, are based on the established treatment of the diffusion of isolated atoms. In the β-aluminas it is clear that ion hopping is a co-operative event, involving many neighbouring ions, and the way that the net hopping rate is determined needs considerable clarification. It is hoped that realistic molecular dynamics simulations, of the type recently completed for sodium–β''-alumina [37], will provide some insight into this problem and others concerning the dynamics of ions in high-density systems.

References

1. R. D. ARMSTRONG, T. DICKINSON and P. M. WILLIS, *Electroanalytical Chem. Interfacial Electrochem.* **53** (1974) 389.
2. D. P. ALMOND, A. R. WEST and R. J. GRANT, *Solid State Commun.* **44** (1982) 1277.
3. D. P. ALMOND, G. K. DUNCAN and A. R. WEST, *Solid State Ionics* **8** (1983) 159.
4. R. M. HILL and A. K. JONSCHER, *J. Non-Cryst. Solids* **32** (1979) 53.
5. C. C. HUNTER, PhD thesis, Aberdeen University (1981).
6. A. K. JONSCHER, *Phys. Thin Films* **11** (1980) 232.
7. R. A. HUGGINS, "Diffusion in Solids, Recent Developments", edited by A. S. Nowick and J. J. Burton (Academic Press, London, 1975).
8. D. P. ALMOND and A. R. WEST, *Phys. Rev. Lett.* **47** (1981) 431.
9. S. J. ALLEN, Jr and J. P. REMEIKA, *ibid.* **33** (1976) 1478.
10. M. S. WHITTINGHAM and R. A. HUGGINS, *J. Chem. Phys.* **54** (1971) 4134.
11. A. K. JONSCHER, *Phil. Mag.* **B38** (1978) 587.
12. *Idem, J. Mater. Sci.* **16** (1981) 2037.
13. P. G. BRUCE, A. R. WEST and D. P. ALMOND, *Solid State Ionics* **7** (1982) 57.
14. J. E. BAUERLE, *Phys. Chem. Solids* **30** (1969) 2657.
15. R. M. HILL and A. K. JONSCHER, *Contemp. Phys.* **24** (1983) 75.
16. J. L. BJORKSTAM, P. FERLONI and M. VILLA, *J. Chem. Phys.* **73** (1980) 2932.
17. J. L. BJORKSTAM, M. VILLA and G. C. FARRINGTON, *Solid State Ionics* **5** (1981) 153.
18. G. C. FARRINGTON and J. L. BRIANT, "Fast Ion Transport in Solids", edited by P. Vashishta, J. N.

Mundy and G. K. Shenoy (North Holland, New York, 1979).
19. J. B. BATES, H. ENGSTROM, J. C. WONG, B. C. LARSON, N. J. DUDNEY and W. E. BRUNDAGE, *Solid State Ionics* **5** (1981) 159.
20. I. WYNN JONES, *Electrochim. Acta* **22** (1977) 68.
21. I. M. HODGE, M. D. INGRAM and A. R. WEST, formerly unpublished data (1977).
22. R. J. GRANT, I. M. HODGE, M. D. INGRAM and A. R. WEST, *J. Amer. Ceram. Soc.* **60** (1977) 226.
23. I. M. HODGE, M. D. INGRAM and A. R. WEST, *J. Electroanal. Chem.* **74** (1976) 125.
24. P. B. MACEDO, C. T. MOYNIHAN and R. BOSE, *Phys. Chem. Glass* **13** (1972) 171.
25. D. P. ALMOND and A. R. WEST, *Solid State Ionics* **11** (1983) 57.
26. C. C. HUNTER, M. D. INGRAM and A. R. WEST, *ibid.* 8 (1983) 55.
27. J. O. ISARD, *J. Non-Cryst. Solids* **1** (1969) 235.
28. M. D. INGRAM and C. T. MOYNIHAN, *Solid State Ionics* **6** (1982) 303.
29. R. E. WALSTEDT, R. S. BERG, J. P. REMEIKA, A. S. COOPER, B. E. PRESCOTT and R. DUPREE, "Fast Ion Transport in Solids", edited by P. Vashishta, J. N. Mundy and G. K. Shenoy (North Holland, New York, 1979).
30. J. L. BRIANT and G. C. FARRINGTON, *Solid State Ionics* **5** (1981) 207.
31. A. K. JONSCHER, *Nature* **267** (1977) 673.
32. K. L. NGAI, A. K. JONSCHER and C. T. WHITE, *ibid.* **277** (1979) 185.
33. L. A. DISSADO and R. M. HILL, *Nature* **279** (1979) 685.
34. S. YOSHIKADO, T. OHACHI, I. TANIGUCHI, Y. ONADA, M. WATANABE and Y. FUJIKI, *Solid State Ionics* 7 (1982) 335.
35. S. YOSHIKADO, T. OHACHI and I. TANIGUCHI, in Proceedings of the 4th International Conference on Solid State Ionics, Grenoble 1983, p. 1305.
36. L. A. DISSADO and R. M. HILL, private communication (1983).
37. M. L. WOLF, J. R. WALKER and C. R. A. CATLOW, *Solid State Ionics* **13** (1983) 33.

Received 6 October
and accepted 19 December 1983